

Magnetic Mullite–iron Composite Nanoparticles Prepared by Solid Solution Reduction

Hao Wang,* Tohru Sekino,[†] and Koichi Niihara[†]

State Key Lab of Advanced Technology for Materials Synthesis and Processing, Wuhan University of Technology,
Wuhan 430070, P. R. China

[†]Institute of Scientific and Industrial Research (ISIR), Osaka University, Mihogaoka 8-1, Ibaraki, Osaka 567-0047

(Received November 15, 2004; CL-041369)

Magnetic composite nanoparticles containing iron and mullite were prepared by reduction of sol–gel-made mullite–iron oxide solid solution. The magnetic properties of nanocomposite suggest that a part of the iron particle exists in the superparamagnetic state. TEM observation shows that metal nanoparticles have an intragranular distribution with iron embedded in mullite grains.

As the promise for practical applications such as catalysis, magnetic recording, magnetic fluids, and biomedicine, special attention has been focused on the fabrication and properties of nanometer-sized magnetic iron particles.^{1–3} In general, iron nanoparticles are prepared from soluble precursors with some methods, such as thermal or sonochemical decomposition and electrochemical or chemical reduction,^{4–7} to obtain small particle size by limiting particle growth. By thermal or sonochemical decomposition of iron pentacarbonyl in the presence of organic surfactants/dispersants (such as oleic acid or polymers), inorganic–organic nanocomposites with the dispersion of iron nanoparticles were prepared. Moreover, the dispersion of iron nanoparticles in inorganic matrixs was also obtained by chemical reduction of iron oxide-contained amorphous silica. Particle growth of iron is controlled by restricting particle formation to confined volumes such as micelles and vesicles or by stabilizing the growing particles with surfactants and dispersants. Actually, ceramic grains can also be used as effective dispersants for preparation of metal nanoparticles by chemical reduction of ceramic solid solution.⁸ Since metal nanoparticles nucleate and grow inside ceramic grains, the particle growth is restricted. Therefore, it becomes possible to prepare intragranular nanocomposite with iron nanoparticles embedded in ceramic grains by chemical reduction of iron oxide-contained solid solution.

Mullite ($3\text{Al}_2\text{O}_3 \cdot 2\text{SiO}_2$) is widely researched for high-temperature structural, electronic, and optical applications.⁹ In addition to the replacement of Si^{4+} and Al^{3+} that leads to the formation of nonstoichiometric compound, mullite can also incorporate different amounts of transition metal cations.¹⁰ In the case of Fe-doped mullite, 12 wt % Fe_2O_3 can be dissolved in mullite matrix under 1200°C by replacing the Al^{3+} at octahedral site.¹¹ We believe that this is the first report on the fabrication and magnetic property of monodisperse air-stable α -Fe nanoparticles embedded in mullite grains by hydrogen reduction of mullite–iron oxide solid solution. The process involves the preparation of oxide solid solution through sol–gel method and reduction by hydrogen flow gas.

To synthesize mullite–iron oxide solid solution with nominal composition of $\text{Al}_{5.4}\text{Fe}_{0.6}\text{Si}_2\text{O}_{13}$, $\text{Al}(\text{NO}_3)_3 \cdot 9\text{H}_2\text{O}$, $\text{Fe}(\text{NO}_3)_3 \cdot 9\text{H}_2\text{O}$, and $\text{Si}(\text{OC}_2\text{H}_5)_4$ were used as the precursors for alumina, iron oxide, and silica, respectively. After dissolving

$\text{Al}(\text{NO}_3)_3 \cdot 9\text{H}_2\text{O}$ and $\text{Fe}(\text{NO}_3)_3 \cdot 9\text{H}_2\text{O}$ into ethanol, the solution was stirred and refluxed at 60°C for 12 h and then $\text{Si}(\text{OC}_2\text{H}_5)_4$, premixed with ethanol, was added dropwise. The solution was continuously stirred for another 12 h whereafter pH value of solution was adjusted to 7 by adding ammonia slowly. Gel was collected and washed several times by ethanol and dried in rotary evaporator at 60°C . Dried powders were treated at 500°C for 2 h in the air to remove volatile substance and were successively calcinated at 1200°C for 4 h to form solid solution. To obtain the iron-dispersed mullite nanocomposite powder, solid solution powders were reduced by flowing hydrogen gas at 1300°C for 1 h. Reduced powders were washed by 1 M HNO_3 at 80°C for 1 h to eliminate the intergranular iron particles. The crystalline phases of samples before and after reduction were recorded by a Rigaku RU-200B X-ray diffractometer with 50 kV and 200 mA using $\text{Cu K}\alpha$ radiation. The microstructure of nanocomposite powders was observed by a transmission electron microscope, Hitachi H-8100T. Measurement of magnetic properties was conducted on a Quantum Design MPMS superconducting quantum interference device (SQUID) magnetometer. Zero-field-cooled and field-cooled magnetizations were determined with an applied field of 100 Oe between 10 and 300 K.

XRD patterns of heat-treated powders at 500, 1200°C , along with those of reduced powders before and after acid washing, are shown in Figure 1. Powders remain amorphous after treatment at 500°C , while volatile impurities have been completely eliminated. Through crystallization and reaction of oxide precursors, the mullite–iron oxide solid solution is the only phase detected by XRD after soaking at 1200°C . The peaks of α -Fe appear both in the reduced samples before and after acid

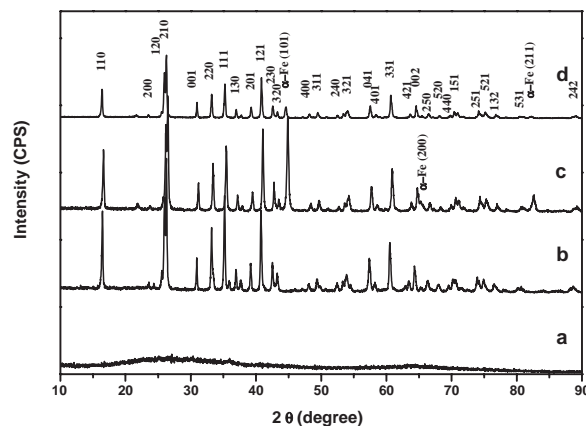


Figure 1. XRD profiles of powders heat-treated at various temperatures and atmosphere. ((a) 500°C , 2 h, air; (b) 1200°C , 4 h, air; (c) 1300°C , 1 h, H_2 ; (d) 1300°C , 1 h, H_2 , acid washing).

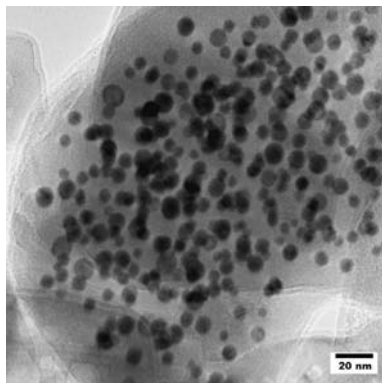


Figure 2. TEM photograph of the sample reduced at 1300 °C and washed in 1 M HNO₃ for 1 h.

washing. It should be noted that the reduction temperature for the formation of iron phase is 1300 °C, which is much higher than that of silica–iron nanoparticles (around 500 °C¹²). Since the iron cation locates in the lattice of mullite, high temperature is essential to supply enough reduction and diffusion ability of hydrogen to obtain iron phase. The intensity decrease of α -Fe peaks after acid washing means that intergranular iron particles are dissolved by acid. The remainder of iron phase after acid washing implies that the mullite grains act as an effective matrix to separate iron phase from the corrosion of acid. Figure 2 shows the typical TEM microstructure of mullite–iron nanocomposite particles. It clearly shows that the monodispersion iron nanoparticles, which are small and dark grains, were embedded in the grain of mullite. The size of the iron nanoparticles is estimated to be 8.2 ± 1.7 nm by TEM image analysis. Therefore, the iron nanoparticles without aggregation, air oxidation, and acid corrosion are fabricated by formation of the intragranular structure in mullite grains.

In magnetism, the temperature dependence of the magnetization for nanosized magnetic particles reveals typical characteristics of superparamagnetism, showing the blocking temperature (T_B) at which the zero-field-cooled magnetization curve exhibits a cusp.¹³ The magnetization versus temperature and field was measured for acid-washed sample in powder form without any substrate. Magnetic moment versus temperature in the temperature range 10–300 K was measured in the zero-field-cooled experiment where the initial field was set to zero as the sample was cooled to the lowest temperature. The field $H = 100$ Oe was then turned on and the magnetic moment versus temperature was measured as the sample was heated from 10 to 300 K. In the field-cooled experiment the field $H = 100$ Oe was applied at 300 K and the magnetic moment was measured as the sample was cooled to the lowest temperature of 10 K. Figure 3 shows the result of magnetization versus temperature for these experiments. It is found that a maximum appears at around 90 K in the zero-field-cooled curve, which is the blocking temperature. However, the zero-field-cooled and field-cooled magnetization curves do not completely overlap with each other above 90 K, which means that some iron nanoparticles are in the state of ferromagnetism. As known, the magnetic behavior of metal nanoparticles is tightly related with their particle size. In the case of iron nanoparticle, the critical size of superparamagnetism is

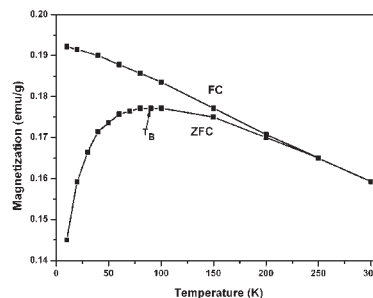


Figure 3. The field-cooled and zero-field-cooled curves of the sample reduced at 1300 °C and washed in 1 M HNO₃.

18 nm.¹⁴ From the result of TEM, the aggregation of some iron particles was observed, which results in the existence of ferromagnetic response at temperature above T_B .

To sum up, we have successfully synthesized the mullite–iron composite nanoparticles through the reduction of sol–gel-prepared mullite–iron oxide solid solution under high temperature. Iron nanoparticles are embedded in the mullite grains to form the intragranular type nanocomposite. With the particle size of 8.2 ± 1.7 nm, a part of iron nanoparticles show the superparamagnetic behavior with the blocking temperature around 90 K.

H. Wang thanks the National Natural Science of China (Grand No. 5010203) in part for financial support.

References

- 1 S. Sun, S. Andres, H. F. Hamann, J.-U. Tiele, J. E. E. Baglin, T. Thomson, E. E. Fullerton, C. B. Murray, and B. D. Terris, *J. Am. Chem. Soc.*, **124**, 2884 (2002).
- 2 J. Chatterjee, Y. Haik, and C.-J. Chen, *J. Magn. Magn. Mater.*, **246**, 382 (2003).
- 3 M. Matsumoto and Y. Miyata, *J. Appl. Phys.*, **91**, 9635 (2002).
- 4 S. H. Sun, C. B. Murray, D. Weller, L. Folks, and A. Moser, *Science*, **287**, 1989 (2000).
- 5 K. S. Suslick, M. Fang, and T. Hyeon, *J. Am. Chem. Soc.*, **118**, 11960 (1996).
- 6 D. E. Weisshaar and T. Kuwana, *J. Electroanal. Chem.*, **163**, 395 (1984).
- 7 H. Perez, J. P. Pradeau, P. A. Albouy, and J. Perez-Omil, *Chem. Mater.*, **11**, 3460 (1999).
- 8 V. Carles, Ch. Laurent, M. Brieu, and A. Rousset, *J. Mater. Chem.*, **9**, 1003 (1999).
- 9 I. A. Aksay, D. M. Dabbs, and M. Sarikaya, *J. Am. Ceram. Soc.*, **74**, 2343 (1991).
- 10 J. Parmentier and S. Vilminot, *J. Alloys Compd.*, **264**, 136 (1998).
- 11 S. P. Chaudhuri and S. K. Patra, *J. Mater. Sci. Lett.*, **35**, 4735 (2000).
- 12 P. Tartaj, T. González-Carreño, O. Bomati-Miguel, and C. J. Serna, *Phys. Rev. B*, **69**, 094401 (2004).
- 13 M. Yoon, Y. M. Kim, Y. Kim, V. Volkov, H. J. Song, and I. W. Park, *J. Magn. Magn. Mater.*, **265**, 357 (2003).
- 14 Y. C. Guo, "Iron Magnetism," People's Education Press, Beijing (1965).